NANO LETTERS

2007
Vol. 7, No. 12
3770−3773

Three-Dimensional Imaging of Carbon Nanotubes Deformed by Metal Islands

Judy J. Cha,*,† Matthew Weyland,†,§ Jean-Francois Briere,‡ Ivan P. Daykov,‡ Tomás A. Arias,‡ and David A. Muller†

School of Applied and Engineering Physics, Department of Physics, Cornell University, Ithaca, New York 14853, and Monash Centre for Electron Microscopy, Building 81, Monash University, VIC 3800, Australia

Received September 4, 2007; Revised Manuscript Received October 25, 2007

ABSTRACT

We report the first direct three-dimensional observations of the buried interface between nanotubes and metal contacts and show that nanotubes can be deformed by the contacts, especially when the metals island rather than wet to nanotubes. Because deforming a nanotube can alter its electronic properties, the islanding metal contacts can introduce additional resistance terms beyond the already present Schottky barrier. The popular contact metal, palladium, lies on the margin between wetting and islanding, suggesting a strategy to improve the contact resistance by alloying.

Challenging the widespread application of carbon nanotubes[1] in electronic devices[2,3] is the high-contact resistance between the nanotubes and metal leads. It varies very widely, increasing exponentially as the nanotube shrinks in diameter.[4,5] Although the physics of the metal−nanotube contact has been investigated theoretically,[6−9] experimental studies on the microscopic contact geometry and its influence on the electrical resistance are lacking. Here, we report on the first direct study of the contact geometry between metals and nanotubes, using annular dark-field (ADF) electron tomography[10] with a scanning transmission electron microscope (STEM) at nanometer resolution.

A good electrical contact between a metal and a nanotube is ensured by minimizing the Schottky barrier at the metal−nanotube contact[6,8,9] and by ensuring that the atoms of the metal and the nanotube are brought into close registration. Given the incommensurate interface between graphite and most metal planes, this is a challenging problem even with flat graphene sheets, but accommodating an interface with the curvature and chirality of a nanotube will add a new degree of complexity. What would be the equilibrium shape of a nanotube in contact with a metal? A number of possible contact geometries can be expected. The metal may wet to the nanotube, resulting in a good physical contact. Or the metal may facet, either leaving voids along the contact surface or deforming the nanotube to accommodate these facets. The resulting geometric distortions in the latter case will have consequences for the electronic structure of nanotube devices.

Depending on the metal, both wetting and nonwetting (islanding) contacts to nanotubes can occur,[11] which results in different equilibrium shapes of the nanotubes. In the wetting case, we find that the metal conforms to the nanotube, and the original shape of the tube is preserved. In the islanding case, the nanotube can be significantly deformed at as well as surrounding the regions in contact with the metal. An elastic theory is used to analytically model the deformation of the nanotubes in the islanding case and identify key terms in the energy balance between wetting and deformation. Furthermore, density functional theory (DFT) calculations are carried out to find that a fully relaxed single-walled nanotube on a flat metal plate is deformed in agreement with our experimental observations and the analytic theory. In formulating a simple scaling argument, we find that the binding energy of the metal to the nanotube is a useful predictor in determining whether the metal will wet or island. Thus, we conducted a systematic study of how the contact geometry varies with the propensity to wet by reconstructing nanotubes of various sizes in contact with different metals at nanometer resolution. We find that as we go from poorly wetting gold (Au), to Au−palladium (Au−Pd) alloy, Pd, and finally strongly wetting titanium (Ti) contacts, a decreasing tendency for nanotubes to deform is observed.

The specimens were prepared by electron-beam evaporating metals onto commercially purchased nanotubes that were dispersed on a holey carbon support film. The geometry of

* Corresponding author. E-mail: jc476@cornell.edu.
† School of Applied and Engineering Physics, Cornell University.
‡ Department of Physics, Cornell University.
§ Monash Centre for Electron Microscopy, Monash University (also present address).

10.1021/nl072251c CCC: $37.00
Published on Web 11/07/2007

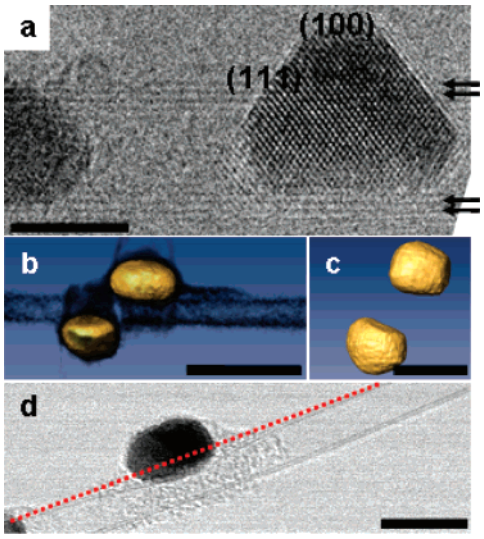

Figure 1. Carbon nanotubes with Au islands. (a) Phase contrast TEM image of a Au island on a triple-walled nanotube. The side walls of the nanotube are indicated with black arrows. The atom registry of the Au island is aligned along the axial direction of the nanotube. (b,c) Views from a tomographically reconstructed nanotube (different from the one shown in (a)) using ADF-STEM images. Yellow, iso-intensity surface, and black, volume render, in (b) denote the Au and the nanotube respectively. (d) This shows a nanotube is kinked at the contact region with a Au island. The red dotted line shows how much the nanotube deviates from a straight line. A contamination layer is also observed around the Au island. Scale bars = 5 nm in (a); 20 nm in (b); 10 nm in (c); and 10 nm in (d).

the high-surface energy Au contacts was examined first. Figure 1a shows at atomic resolution that Au forms strongly faceted islands on nanotubes. Yet, from such two-dimensional (2D) images it is unclear how this faceting is accommodated at the curved surface of the nanotube. The results of the 3D tomographic study (see Supporting Information for more details) of the buried Au-nanotube interface of a separate tube, Figure 1b,c, reveal what is apparently a flat contact surface. This implies that the nanotube has undergone significant radial deformation to accommodate the faceting of the Au contact. The faceting of the Au clusters and the resultant flat contact surfaces are observed universally in all reconstructed nanotubes in contact with Au, although single-walled nanotubes tend to deform more than multiwalled nanotubes. In addition, a kink along the nanotube, Figure 1d, is sometimes observed at the contact region, which is similar to nanotube deformation induced by atomic force microscopy (AFM) tips.[12,13]

The faceting observed in Figure 1c is not atomically sharp because the resolution of the tomographic reconstruction degrades to roughly a nanometer[10] even though the focused probe in STEM is approximately 0.2 nm in diameter. However, because the observed clusters are generally larger than a couple of nanometers, a nanometer resolution is sufficient to observe faceting. Detailed descriptions of the tomography technique, reconstruction method, and the limiting factors on the final resolution are provided in the Supporting Information available online.

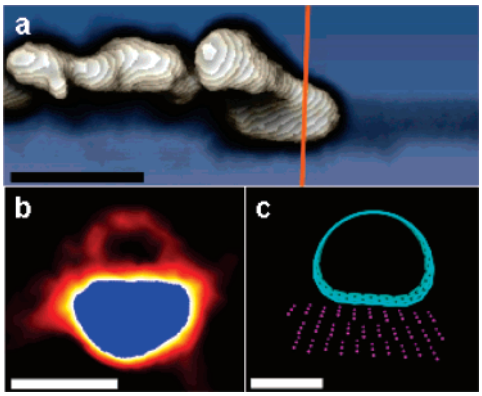

Figure 2. Carbon nanotubes with Au−Pd islands. White and black in (a), iso-intensity surface and volume render, denote the Au−Pd islands and the nanotube, respectively. (b) A cross-section view of the orange slice in (a). From (b), the radial deformation of the nanotube is evident. (c) The DFT calculation of a fully relaxed (20,0) carbon nanotube (blue) on three layers of Pd atoms (pink). Scale bars = 10 nm in (a); 4 nm in (b); 1 nm in (c).

As a material commonly used as a conductive-coating layer in scanning electron microscopy, an alloy of 70% Au and 30% Pd should offer improved wetting. Despite this, the tomographic reconstruction shown in Figure 2a shows that the Au−Pd alloy also forms islands on nanotubes. But unlike the Au, no strong faceting is observed in the Au−Pd islands, whose surface looks rounded in Figure 2a. Nevertheless, a cross-section through the reconstruction, Figure 2b, reveals a relatively flat contact surface and resultant nanotube deformation. This finding is confirmed by DFT calculations of the equilibrium nanotube shape for a (20,0) carbon nanotube in contact with three atomic layers of Pd. Pd was used instead of the Au−Pd alloy to simplify the calculation, and we will shortly compare the calculation to Pd experimental data. The equilibrium shape was reached by fully relaxing the nanotube and the first two Pd layers while the last Pd layer was fixed to be planar to replicate the flat contact surface (see Supporting Information for more details). The cross-section view from the DFT calculation is shown in Figure 2c, and despite the difference in the size of the nanotubes the overall shape of the relaxed nanotube agrees well with the experimental result, Figure 2b, confirming the prediction that nanotubes can deform on a flat surface.[14]

We note that the nanotube in Figure 2b is a multiwalled nanotube while the DFT calculations use a single-walled nanotube. Despite the difference in the number of walls, the essential underlying physics is the same in both the experiments and the DFT calculations, namely achieving balance between the energy needed to deform the circular cross-section of the tube and the amount of energy gained by increasing the contact area. As a result, we expect to see geometrically similar cross-sectional shapes in both cases. However, because a multiwalled nanotube would have a larger bending rigidity in proportion to its number of walls than a single-walled nanotube, the length scales associated with the experimental results are expected to be larger than those of the DFT calculations. In fact, the square-root of the ratio of the bending rigidity to the surface energy of the

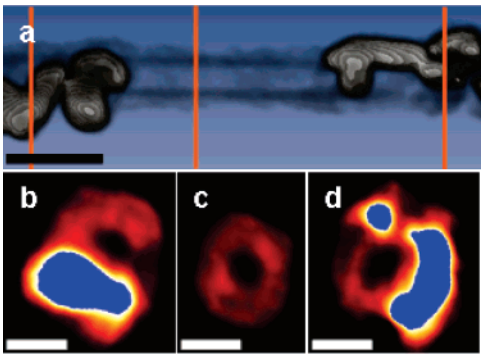

Figure 3. Carbon nanotubes with Pd islands. (a) Volume render of the tomographically reconstructed nanotube (black) with iso-intensity surface of Pd islands (white). (b−d) Cross-section views of the orange slices in (a). Scale bars = 10 nm in (a); 4 nm in (b−d). We note that the diameter (∼5 nm) and the wall thickness (∼1.4 nm) of the nanotube measured from the reconstruction agree very well with those measured from the ADF-STEM images (not shown in the figure) once the lower resolution of tomographic method is taken into account.

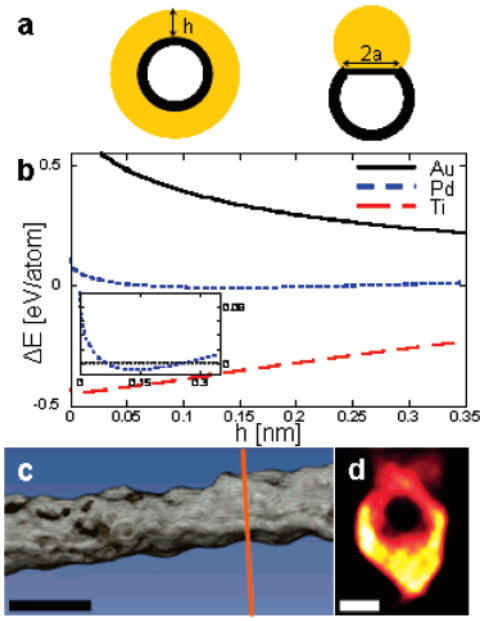

Figure 4. Energy-balance calculation and carbon nanotubes with Ti contacts. (a) A schematic diagram of a wetting and islanding metal (yellow) on a nanotube (black). (b) Energy difference of the two systems per atom, $(E_{tot}(\text{wet}) - E_{tot}(\text{island}))/N_{tot}$, for Au, Pd, and Ti with a nanotube of radius 1 nm. The inset shows only the Pd case. (c) Volume render of a carbon nanotube (black) with iso-intensity surface of Ti wetting layer (white). A little intensity of black exists outside of the Ti-wetting layer, which indicates a thin contamination layer. (d) Cross-section view of the orange slice in (c). Scale bars = 10 nm in (c); 4 nm in (d).

contact sets the only length scale in the problem, other than the initial radius of the tube. An analytical expression, which balances the deformation energy of the nanotube with the contact energy and the surface energy of the metal, is discussed later (more details can be found in the Supporting Information).

Both Au and the Au−Pd alloy form flat contact surfaces; however, pure Pd has a greater tendency to wet. The tomographic reconstruction shown in Figure 3a reveals that Pd also forms islands on nanotubes. That the Pd islands are rounded with no apparent faceting suggests that the Pd may be polycrystalline and the islands may have formed by several smaller islands coalescing together. Interestingly, the cross-sections through the reconstruction, Figure 3b−d, show a slightly curved contact surface. On average, this results in less deformation of nanotubes compared to the Au and Au−Pd cases. However, we find that the degree of nanotube deformation varies widely, due to the widely varying shapes of Pd islands and their coalescence. This implies that pure Pd is still some way from perfectly wetting the nanotube.

The wide range in the degree of nanotube deformation under the Pd islands indicates that the nanotube deformation may be related more to the formation of islands (and their coalescence) than to faceting. Hence, if the metal wets the nanotube continuously the deformation might not occur. The competition between the metal islanding and nanotube deformation can be estimated by balancing the anisotropic free-surface energy of the metal and the contact-surface energy at the interface against the deformation energy of the nanotube. By summing the energy terms, the total energy of the two extremes, a completely wetting system or an islanding system, is obtained. Although approximate, this calculation helps to identify a general wetting trend for different metals on nanotubes.

The assumed geometries for the ideal wetting and islanding systems are shown in Figure 4a, where the cross-sectional area of the metal is the same for both systems. We calculate the total energy (E_{tot}) of the systems as a function of the contact and remaining surface area, S_c and S_s, respectively, as

$$E_{tot} = \frac{2\pi^2 DL}{\pi R - a} + (u_{fc} - u_{bc})\sigma S_c + u_{fs}\sigma S_s \qquad (1)$$

where D is the effective bending stiffness of the nanotube, L is the length of the deformed region of the nanotube, R is the radius of the nanotube, σ is the number density of the metal per unit area, u_{fc} is the free-surface energy of the contact surface per atom, u_{fs} is the free-surface energy of the remaining surface per atom, and u_{bc} is the binding energy of the metal to the nanotube per atom. The energy unit for E_{tot} is eV. Note that as the cross-sectional area is conserved, the volume energy of the metal is identical for both systems per given metal and thus cancels out. The first term in eq 1 is the deformation energy of the nanotube based on an elastic theory.[15−17] A more detailed calculation of eq 1 is provided in Supporting Information available online.

We used eq 1 to calculate E_{tot} for the two ideal systems for each metal contact and obtained the energy difference per atom, $\Delta E = (E_{tot}(\text{wet}) - E_{tot}(\text{island}))/N_{tot}$ where N_{tot} is the total number of surface atoms for a given metal contact. If ΔE is negative, then the metal would wet nanotubes rather than form islands. Shown in Figure 4b are plots of ΔE with increasing thicknesses of deposited Au, Pd, and Ti for a single-walled nanotube with radius of 1 nm. From Figure 4b, Au would always island while Ti would wet. Palladium lies between the two systems. Its ΔE crosses zero and

remains close to zero for a wide range of nanotube diameters, which indicates partial wetting. Experimentally, the curved contact surface, as shown in Figure 3d, might suggest that Pd partially wets nanotubes. From the inset in Figure 4b, which shows ΔE for Pd, the predicted thickness of the wetting layer for Pd is about a monolayer. At atomic scale, the simple energy-balance argument using bulk properties cannot accurately model the system; hence ab initio calculations are required to accurately predict the thickness of the wetting layer for Pd.

It is worth noting that estimates of the nanotube deformation energy[16] and DFT calculations[8] suggest that the energy cost of nanotube deformation is negligible[14] until the radius of curvature falls below a few angstroms. For all but the smallest nanotubes (which will not deform), eq 1 suggests that it is largely the binding energy of the metal to the nanotube (with respect to the free-surface energy of the metal) that governs the wettability of the metal to the nanotube. According to DFT calculations within the generalized gradient approximation,[18] of the three metals under study, Ti has the highest binding energy to the nanotube, 2.9 eV/atom, while Au has the lowest, 0.6 eV/atom. Hence, creating a large contact surface by wetting lowers the total energy of the system significantly for Ti but not appreciably for Au. The binding energy of Pd is 1.7 eV/atom,[18] which is fairly high. But the free-surface energy of Pd, which the same type of calculation gives to be approximately 1.0 eV/atom,[19] prevents Pd from making a large free surface. Therefore, complete wetting does not occur for Pd even though the binding energy is high.

Because eq 1 predicts wetting for Ti contacts, Ti is studied here as an example of a material with good wetting characteristics despite the high Schottky barrier between Ti and a nanotube, which leads to a bad electrical contact. The tomographic reconstruction, Figure 4c, shows that Ti covers the nanotube uniformly, strongly indicating complete wetting. A cross-section view, Figure 4d, reveals that Ti wraps around the nanotube and preserves its round shape. The wetting by Ti is observed universally regardless of the nanotube size.

As both theoretical calculations and experimental observations show band gap changes due to mechanical nanotube deformation by AFM tips,[12,13,20−22] the observed deformations by the poorly wetting contacts imply that the electronic structure of the nanotube may change significantly upon putting an electrical contact to it. Therefore, in addition to a Schottky barrier at the contact, a geometrically induced scattering term can also be expected. Hence, promising contact metals for nanotube devices must have good wettability to nanotubes as well as a small Schottky barrier. The popular contact metal, Pd, comes close to satisfying this condition and we anticipate that alloys of Pd, which possess a lower free-surface energy than pure Pd, may provide improved contacts both physically and electrically.

Acknowledgment. We are grateful to Professor Jim Sethna for his valuable discussions on balancing the energy terms of the metal islands and the nanotubes. We are also grateful to Professor Paul McEuen and Arend van der Zande for the use of their furnace and discussions. We acknowledge use of the FEI Tecnai F20-STEM administered by John Grazul, facility manager. We are grateful to the Cornell NanoScale Science and Technology Facility (CNF) for the E-beam evaporator. This work has been supported by the Cornell Center for Materials Research (CCMR) IRG-A.

Supporting Information Available: Discussion of electron tomography experiments; discussion of DFT calculations; detailed derivation of eq 1; a movie showing a 3D reconstruction of a nanotube with faceted Au islands. This material is available free of charge via the Internet at http://pubs.acs.org.

References

(1) Iijima, S. *Nature* **1991**, *354*, 56−57.
(2) Tans, S. J.; Verschueren, A. R. M.; Dekker, C. *Nature* **1998**, *393*, 49−52.
(3) Sazonova, V.; Yaish, Y.; UstUnel, H.; Roundy, D.; Arias, T. A.; McEuen, P. L. *Nature* **2004**, *431*, 284−287.
(4) Kim, W.; Javey, A.; Tu, R.; Cao, J.; Wang, Q.; Dai, H. *Appl. Phys. Lett.* **2005**, *87*, 173101−3.
(5) Chen, Z.; Appenzeller, J.; Knoch, J.; Lin, Y. M.; Avouris, P. *Nano Lett.* **2005**, *5*, 1497−1502.
(6) Heinze, S.; Tersoff, J.; Martel, R.; Derycke, V.; Appenzeller, J.; Avouris, P. *Phys. Rev. Lett.* **2002**, *89*, 106801.
(7) Zhu, W.; Kaxiras, E. *Nano Lett.* **2006**, *6*, 1415−1419.
(8) Shan, B.; Cho, K. *Phys. Rev. B* **2004**, *70*, 233405.
(9) Nemec, N.; Tomanek, D.; Cuniberti, G. *Phys. Rev. Lett.* **2006**, *96*, 076802−4.
(10) Midgley, P. A.; Weyland, M. *Ultramicroscopy* **2003**, *96*, 413−431.
(11) Zhang, Y.; Dai, H. *Appl. Phys. Lett.* **2000**, *77*, 3015−3017.
(12) Tombler, T. W.; Zhou, C.; Alexseyev, L.; Kong, J.; Dai, H.; Liu, L.; Jayanthi, C. S.; Tang, M.; Wu, S.-Y. *Nature* **2000**, *405*, 769−772.
(13) Minot, E. D.; Yaish, Y.; Sazonova, V.; Park, J.-Y.; Brink, M.; McEuen, P. L. *Phys. Rev. Lett.* **2003**, *90*, 156401−4.
(14) Hertel, T.; Walkup, R. E.; Avouris, P. *Phys. Rev. B* **1998**, *58*, 13870−13873.
(15) Robertson, D. H.; Brenner, D. W.; Mintmire, J. W. *Phys. Rev. B* **1992**, *45*, 12592−12595.
(16) Tang, T.; Jagota, A.; Hui, C.-Y. *J. Appl. Phys.* **2005**, *97*, 074304.
(17) Yakobson, B. I.; Brabec, C. J.; Bernholc, J. *Phys. Rev. Lett.* **1996**, *76*, 2511−2514.
(18) Durgun, E.; Dag, S.; Bagci, V. M. K.; Gulseren, O.; Yildirim, T.; Ciraci, S. *Phys. Rev. B* **2003**, *67*, 201401−4.
(19) Vitos, L.; Ruban, A. V.; Skriver, H. L.; Kollar, J. *Surf. Sci.* **1998**, *411*, 186−202.
(20) Gomez-Navarro, C.; Saenz, J. J.; Gomez-Herrero, J. *Phys. Rev. Lett.* **2006**, *96*, 076803.
(21) Shan, B.; Lakatos, G. W.; Peng, S.; Cho, K. *Appl. Phys. Lett.* **2005**, *87*, 173109−3.
(22) Park, C.-J.; Kim, Y.-H.; Chang, K. J. *Phys. Rev. B* **1999**, *60*, 10656.

NL072251C